Available online at www.sciencedirect.com
SCIENCE DIRECT®
Optics Communications 254 (2005) 290–298
OPTICS COMMUNICATIONS
www.elsevier.com/locate/optcom

Amplification of narrow line LiF : F_2^{+**} color center laser oscillation

Amelia G. VanEngen Spivey, Vladimir V. Fedorov, Michael M. McKerns [1], Christopher M. Lawson, Sergey B. Mirov *

Department of Physics, University of Alabama at Birmingham, CH 310, 1530 Third Avenue South, Birmingham, AL 35294-1170, United States

Received 11 November 2004; received in revised form 8 March 2005; accepted 26 May 2005

Abstract

A nanosecond pulsed LiF : F_2^{+**} color center master oscillator and power amplifier scheme is presented. Maximum amplified pulse energies of ~15 mJ near 930 nm are achieved, with an amplification gain of more than 35× under less than 50 mJ of absorbed pump energy. Furthermore, flexibility in the amplifier design should allow for additional improvements through steps such as saturating the passive losses in the crystal. We also discuss the optimization of color center crystal preparation, which has facilitated the growth of LiF : F_2^{+**} color center crystals with large absorption coefficients (from 2 to 8 cm^{-1} at the maximum near 600 nm). Passive losses in these crystals are estimated to be less than 0.08 cm^{-1} at the oscillation wavelength and are attributed to the presence of "F_2^{+**}-like" color centers.

PACS: 42.60.Da; 42.60.Ln; 42.70.Hj; 61.72.Ww; 78.55.Fv; 81.40.Tv; 82.50.Kx

Keywords: Color center laser; LiF : F_2^{+**}; Laser amplifier; Tunable laser; Efficiency; Gain; Passive losses

1. Introduction

Lasers based on LiF crystals containing stabilized F_2^{+**} color centers (CCs) are efficient and reliable sources of tunable near-infrared radiation [1,2]. As is the case with most color centers, F_2^+ CCs are point defects produced by ionizing radiation. The F_2^+ CCs are formed when an electron becomes trapped by two adjacent anion vacancies

* Corresponding author. Tel.: +1 205 9345318; fax: +1 205 9348042.
E-mail addresses: spivey@phy.uab.edu (A.G. VanEngen Spivey), mirov@uab.edu (S.B. Mirov).
[1] Present address: Division of Engineering and Applied Sciences, California Institute of Technology, Pasadena, CA 91125, United States.

0030-4018/$ - see front matter © 2005 Elsevier B.V. All rights reserved.
doi:10.1016/j.optcom.2005.05.045

with axial symmetry along the (1 1 0) direction [3], and exhibit some very favorable optical properties. For example, the F_2^+ CCs are characterized by a high quantum efficiency of luminescence at room temperature and have large absorption and luminescence cross-sections ($\sim 5.7 \times 10^{-17}$ cm^2). In addition, the wide absorption band (500–800 nm) of F_2^+ CCs makes possible the use of a variety of pumping sources, such as ruby lasers, alexandrite lasers, diode lasers, and the second harmonic of the Nd:YAG laser. However, F_2^+ CCs in undoped LiF are thermally unstable at room temperature with a decay time of ~12 h [3].

To increase the thermal stability of F_2^+ CCs, Khulugurov and Lobanov [4] suggested co-doping LiF crystals with suitable anion or cation impurities. Impurity doping has proven to be a key component of creating stable color centers in LiF. Specifically, γ-irradiation of LiF doped with OH^- and Mg^{2+} impurities results in the formation of F_2^+–O^{2-}/Mg^{2+} complexes (F_2^{+**} centers). The F_2^{+**} color centers are stable at room temperature over periods of months and even years, making them suitable for use in laser development. Recently, progress in the development of stable LiF : F_2^{+**} CC crystals resulted in the design of a nanosecond-pulsed laser with an efficiency of 58% for operation at room temperature and tunable over the 800–1200 nm spectral range [1]. The work presented here is motivated by the desire to increase the energy of pulses emitted by a tunable nanosecond LiF : F_2^{+**} laser for use in nonlinear optics and excited-state absorption measurements. The typical method used to obtain high-energy output pulses from a tunable LiF : F_2^{+**} CC laser is to increase the pump energy. Unfortunately, under high-energy pumping, it is difficult to maintain the spectrally-narrow laser output due to non-wavelength-selective amplification of superluminescence (i.e., amplified spontaneous emission). Theoretically, the wavelength-selectivity of the cavity can be improved by decreasing the Fresnel number of the cavity, either by decreasing the pump beam size in the laser crystal or by increasing the cavity length. However, at high pumping energies, decreasing the pump beam size can lead to optical damage of the crystal, and increasing the cavity length typically increases the oscillation build-up time and decreases the laser efficiency.

An alternate method for achieving high-energy output pulses with favorable spatial and spectral characteristics is to employ a two-stage laser oscillator and amplifier. The use of a master oscillator and a power amplifier (MOPA) scheme is standard practice in laser systems where high output powers are required [5]. For example, the MOPA scheme has been used to increase the output power of dye lasers using either single-pass or multi-pass power amplifiers [6–10]. Using color center crystals, amplification of the output of a diode laser in a LiF : F_2^{+**} CC crystal was achieved by Basiev and co-workers [11,12]. In their work, a LiF : F_2^{+**} CC crystal amplifier was seeded with the narrow-band output of a diode laser at 900 nm. They achieved 300-fold magnification of the diode laser radiation in single pass amplification, but due to very low seeding energy the total output energy was only 40 nJ.

To our knowledge, we present in this paper the first high-energy amplification of the output of a tunable LiF : F_2^{+**} CC laser using a LiF : F_2^{+**} CC amplifier crystal. This two-stage oscillator–amplifier is designed to yield pulse energies suitable for nonlinear optical applications while maintaining the spatial and spectral output characteristics of the tunable LiF : F_2^{+**} CC laser. We also discuss two related issues: preparation of the stabilized LiF : F_2^{+**} color center crystals and passive losses in LiF : F_2^{+**} color center lasers at the oscillation wavelength due to the presence of F_2^{+**}-like color centers. Passive losses due to the F_2^{+**}-like color centers may ultimately limit the performance of the LiF : F_2^{+**} laser amplifier. However, by optimizing the amplifier design it should be possible to achieve even higher pulse energies than are presented here.

2. Crystal preparation

The preparation of stable LiF : F_2^{+**} color center crystals is a crucial part of laser design. Preparation of these crystals is described in detail elsewhere [1], but in general it is carried out as follows. LiF crystals with different impurities (Mg, OH, and LiO_2)

essential for stabilization of F_2^{+**} centers were grown from the melt using the Czochralski method. In order to obtain a high concentration of F_2^{+**} centers and a small concentration of colloids and parasitic aggregate color centers, LiF crystals doped with LiOH and MgF_2 were subjected to a multistep Co^{60} γ-irradiation treatment with a dose up to 10^8 R. The crystals are then stored at room temperature for a period of several months.

The physical processes that lead to formation of stable F_2^{+**} color centers in LiF crystals are widely understood and are discussed in detail elsewhere [1,3]. We discuss some of the specific mechanisms here and present some new data related to crystal preparation. First, there are processes that occur during the ionizing radiation treatment, such as dissociation of the OH impurities according to [13]

$$OH^- \xrightarrow{h\nu} O^- + H \tag{1}$$

or

$$2(OH)^- \xrightarrow{h\nu} O_2^- + e^- + V_a^+ + 2H. \tag{2}$$

In order to measure the concentration of LiOH impurities, which determines the optimal radiation dose for each crystal, absorption measurements were conducted on each LiF crystal.

The presence of OH^- impurities in LiF creates an absorption band centered at 2680 nm. The absorption spectra of two different LiF:LiOH crystals in the near IR spectral region are shown in Fig. 1(a) and (b). Fig. 1(c) shows that the OH^- absorption band is greatly diminished after γ-irradiation of the crystals with a dose of 2.4×10^7 R. This suggests that a dose of 2.4×10^7 R is sufficient for nearly complete destruction of the hydroxyl group. The destruction of the hydroxyl group and formation of the products of mechanisms (1) and (2) are essential for formation of stable, positively charged F_2^{+**} centers via [3]

$$O^- + e^- + V_a^+ \rightarrow V_a^+ O^{2-} \tag{3}$$

followed by

$$V_a^+ O^{2-} + F \rightarrow F_2^+ O^{2-}. \tag{4}$$

The cation impurities are also important. The mechanism for the formation of F_2^{+**}-like CCs by cation impurities in LiF was proposed by Khulugurov and Lobanov [4], as follows. During the

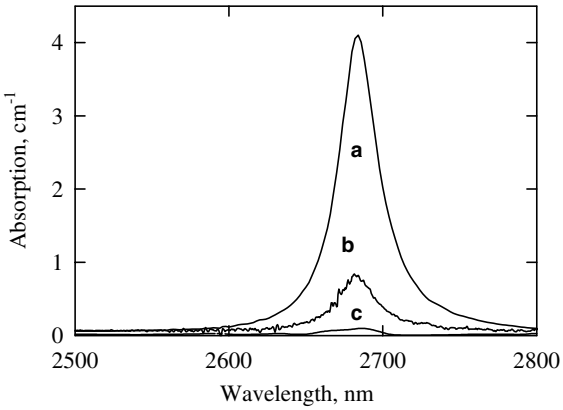

Fig. 1. Infrared absorption spectra of LiF:LiOH crystals. Curves (a) and (b) show spectra for two LiF:LiOH crystals with different concentrations of OH^- impurities. Curve (c) shows the absorption spectrum of the crystal of curve (a) after irradiation with 2.4×10^7 R.

crystal growth process, divalent metals replace Li^+ ions in the lattice. Charge compensation is usually provided by the cation vacancy, V_c^-, located nearest to a given Me^{2+} ion. Interaction between the vacancy-metal dipole and an F center leads to the formation of a singly-ionized metal atom, Me^+, and a pair of anion-cation vacancies according to the following mechanism [1,14]:

$$V_c^- Me^{2+} + F \rightarrow Me^+ + V_a^+ V_c^-. \tag{5}$$

Over a period of time, due to its mobility at room temperature, the $V_a^+ V_c^-$ bi-vacancy can associate with an F center to form a thermally stable F_2^{+**} CC according to

$$V_a^+ V_c^- + F \rightarrow F_2^+ V_c^-. \tag{6}$$

An important issue related to preparation of these crystals is that some of the mechanisms leading to F_2^{+**} CC formation occur on a very long time scale. Of the mechanisms outlined above, mechanisms (4) and (6) both proceed as a result of thermal diffusion processes that are active at room temperature and above. Fig. 2(a) shows the absorption spectrum of a single LiF crystal (doped and γ-irradiated) after storage at room temperature for one month (curve 1), four months (curve 2), and nine months (curve 3). Fig. 2(b) shows the concentration of F_2^{+**} CCs measured in the same LiF crystal at the different time intervals.

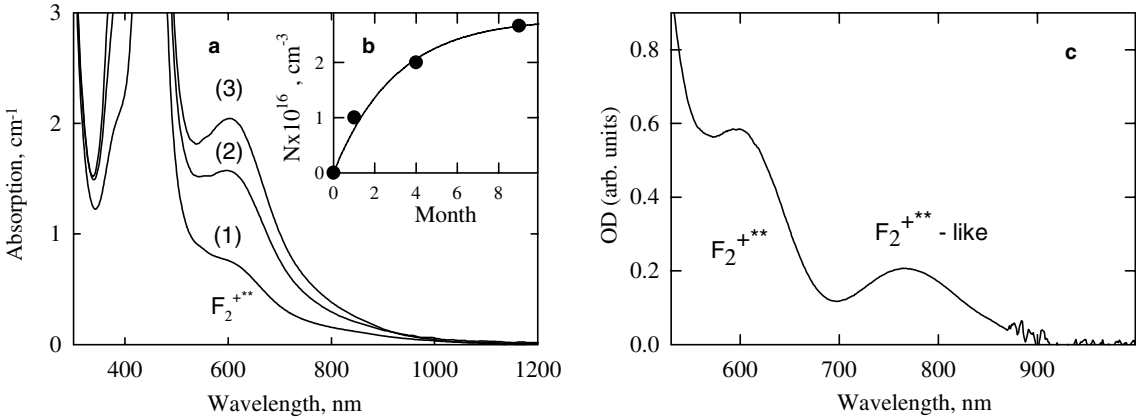

Fig. 2. (a) Absorption spectrum of a LiF crystal irradiated with a total dose of 4.8×10^7 R after one month (curve 1), four months (curve 2) and nine months (curve 3) of storage at room temperature; (b) concentration of F_2^{+**} CCs versus time elapsed after irradiation; (c) difference in absorption spectra of two LiF crystals doped with different stabilization impurities. The absorption due to F_2^{+**}-like CCs is clearly visible centered at 770 nm.

The dynamics of F_2^{+**} CC accumulation at room temperature are fit quite accurately by an exponential curve with an effective time constant of 3 months. The fact that the LiF : F_2^{+**} CC concentration increases with time, rather than decaying, is important for use of these CC crystals in devices over a period of years.

The crystal preparation process above can lead to high concentrations of stable F_2^{+**} CCs in LiF crystals, as evidenced by the large absorption coefficients seen in Fig. 2(a). The maximum absorption coefficient achieved in this study was 8 cm^{-1} at approximately 600 nm. To our knowledge, this is the highest absorption observed to date in LiF:OH crystals, and it serves as evidence of the effectiveness of the coloration process outlined above. Unfortunately, the crystal with the highest absorption coefficient exhibited a prohibitive amount of light scattering. Thus, crystals with smaller absorption coefficients were used in the work presented here.

In addition to the F_2^{+**} CCs described above, additional "F_2^{+**}-like" CCs with an absorption band maximum at 770 nm have been observed in low-temperature studies [15,16]. At room temperature, the absorption band due to the F_2^{+**}-like centers is difficult to resolve due to overlap with the F_2^{+**} absorption band. However, by comparing the absorption spectra of crystals with different concentrations of the various CCs, the absorption due to F_2^{+**}-like centers can be detected. For example, one might compare the absorption spectra of two LiF crystals doped with different stabilization impurities. Fig. 2(c) shows the difference between two such absorption spectra. The F_2^{+**}-like CC band (which peaks at 770 nm and has a linewidth $\Delta\lambda_{\mathrm{FWHM}} = 140$ nm) is clearly visible along with the F_2^{+**} CC absorption band (which peaks near 600 nm). The existence of the F_2^{+**}-like CCs has two major consequences. First, the presence of the F_2^{+**}-like centers increases the long-wavelength tuning range of the CC laser. A second, deleterious, effect is the introduction of additional losses for laser oscillation at long wavelengths. In the next section, we estimate the passive losses due to F_2^{+**}-like CCs when a LiF : F_2^{+**} CC crystal is used as the lasing medium in a simple flat cavity.

3. Estimation of passive losses in the laser crystal

Optical losses in laser cavities depend on the losses in the laser crystal and losses in the other optical components. In the crystal, losses can occur at the pumping wavelength or at the wavelength of laser oscillation. In lasers based on LiF : F_2^{+**} CC crystals, losses at the wavelength of oscillation (centered near 930 nm for a non-

selective cavity) should be much greater than losses at the pumping wavelength (633 nm in this work).

In order to estimate losses in the LiF : F_2^{+**} CC laser crystal at the laser oscillation wavelength, experiments were performed using a non-selective flat-flat laser cavity. Pumping was provided by a 10-Hz repetition rate Q-switched single-frequency Nd:YAG laser emitting pulses of 7-ns duration. The second harmonic of the Nd:YAG laser, at 532 nm, was Raman-shifted in the backscattering geometry using a D_2 Raman cell, yielding 633-nm light that was used to pump the CC laser. The Brewster-cut LiF : F_2^{+**} CC laser crystal was 2.7 cm long with an 8×16 mm clear aperture and maximum absorption of 1.97 cm^{-1} at 600 nm. The total cavity length was 11 cm. The unfocused 633-nm pump beam with diameter 3.5 mm was introduced into the LiF crystal through a dichroic mirror. The input dichroic mirror had 93% transmission at the pumping wavelength and high reflectivity in the 800–1040 nm spectral range. Output couplers with different peak reflectivities were used during the experiment.

The output efficiency of the laser was measured while varying the reflectivity of the output coupler. Fig. 3(a) shows the output energy per pulse as a function of absorbed pump pulse energy for different output couplers, and Fig. 3(b) shows the slope efficiencies calculated from Fig. 3(a) as a function of output coupler reflectivity, R. The maximum slope efficiency for this non-selective cavity was ~34%, which was obtained using an output coupler with $R = 20\%$. However, the slope efficiency is fairly constant between $R = 10\%$ and $R = 60\%$, providing some flexibility in the choice of diffraction grating used for output coupling in a dispersive cavity.

The dependence of the slope efficiency on R can be easily explained. Above $R = 20\%$, the decrease of the slope efficiency with increasing output coupler reflectivity is simply due to the introduction of passive losses in the cavity. Below $R = 20\%$, the decrease of the slope efficiency with decreasing output coupler reflectivity is due to the oscillation build-up time. During the build-up time of the oscillation, the conversion efficiency of the pump energy is low. Low output coupler reflectivity

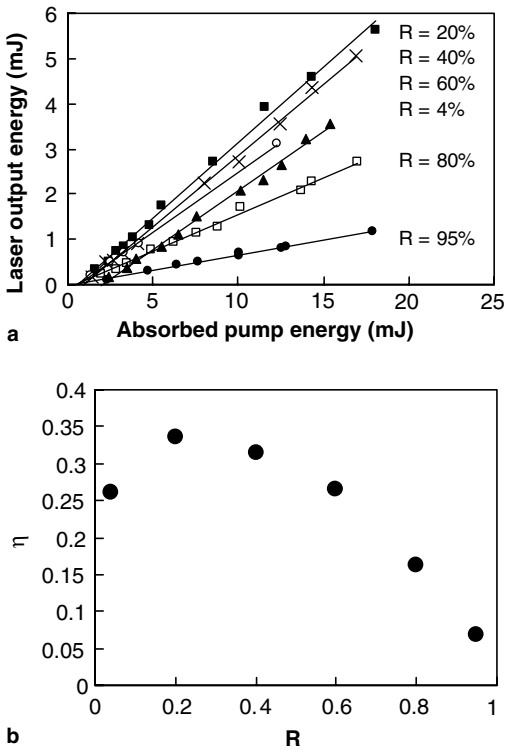

Fig. 3. (a) Laser output energy per pulse versus absorbed pump energy per pulse for the non-selective LiF : F_2^{+**} CC laser with different output couplers. The lines are linear fits to the data. (b) Slope efficiency versus output coupler reflectivity, calculated from the data shown in (a).

(i.e., decreased positive feedback in the laser cavity) increases the build-up time required for oscillation, and therefore decreases the slope efficiency of the lasing process.

Based on the measured slope efficiency as a function of output coupler reflectivity, two types of analysis are used to estimate the losses in the LiF : F_2^{+**} CC laser crystal and the maximum possible slope efficiency for the laser. We analyze only the data taken using output couplers with $R \geqslant 40\%$, since the models used are not appropriate for the case of low output coupler reflectivity and short pump pulses. The first analysis method, proposed by Caird et al. [17], is based on a comparison of inverse slope efficiency ($1/\eta$) versus inverse output coupler transmission ($1/T$), where $T = 1 - R$. Fig. 4(a) shows such a plot for the data in Fig. 3. The round trip cavity losses ($L = 2\delta l$,

where l is the length of the lasing medium and δ represents the loss per unit length) and the maximum intrinsic slope efficiency (η_0) can be calculated using [17]

$$\frac{1}{\eta} = \frac{1}{\eta_0}\left(1 + \frac{L}{T}\right). \tag{7}$$

By fitting the experimental data in Fig. 4(a) with this expression, we find that the losses in the crystal at the wavelength of laser emission are given by $\delta = 0.05\ \text{cm}^{-1}$. The corresponding maximum intrinsic slope efficiency is $\eta_0 = 0.41$, or 41%. The maximum measured slope efficiency of 34% compares fairly well with this theoretical maximum slope efficiency.

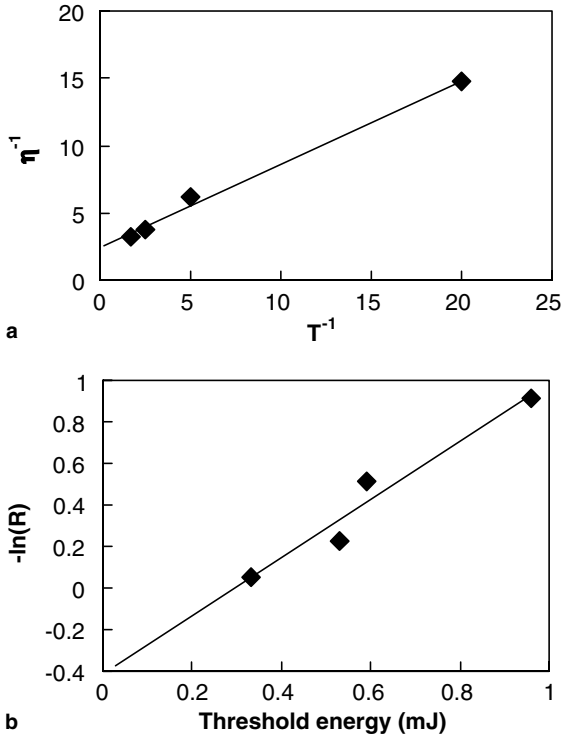

Fig. 4. (a) Inverse slope efficiency versus inverse output coupler transmission for a broadband laser cavity with 2.7-cm LiF CC crystal. (b) Plot of $-\ln(R)$ versus lasing threshold energy, where R is the reflectivity of the output coupler, for the same laser cavity as in (a). The solid lines are linear fits to the data. The data in this figure corresponds to the data shown in Fig. 3(a) and (b) for $R \geqslant 40\%$.

The second analysis method, originated by Findlay and Clay [18], consists of plotting the laser threshold energy versus the natural log of the output coupler reflectivity, as shown in Fig. 4(b). In this case, the relationship between the threshold energy, output coupler reflectivity, and crystal losses is given by [18]

$$E_{\text{th}} = E'_{\text{th}}\left(1 - \frac{\ln R}{2l\delta}\right), \tag{8}$$

where R is the output coupler reflectivity (assuming 100% reflectivity of the other cavity mirror) and E'_{th} is the threshold energy for zero output coupling. The crystal loss at the emission wave length calculated using this technique is $\delta = 0.08\ \text{cm}^{-1}$, which is in good agreement with the results obtained above using the Caird analysis. In addition, the Findlay–Clay analysis yields a zero-output-coupling lasing threshold energy $E'_{\text{th}} = 0.3$ mJ.

We believe that the crystal losses in the near infrared calculated using the Caird and Findlay–Clay methods are due to absorption by the F_2^{+**}-like CCs. As shown by Jenkins and co-workers [16], these CCs have some absorption in the near-infrared oscillation region of the LiF : F_2^{+**} CC laser. Due to the weak excitation energies used in the current work, we do not observe saturation of the losses attributed to absorption by F_2^{+**}-like CCs. However, saturation of these losses can be achieved under high energy pumping, as demonstrated by Dergachev and Mirov [1]. In that work, the slope efficiency was larger for pumping energies above 100 mJ compared to the efficiency for low-energy pumping. The increase in slope efficiency at high pumping energy in [1] most likely resulted from saturation of the losses due to F_2^{+**}-like CCs and allowed the authors to achieve a maximum slope efficiency of 58% that was close to the Stokes shift limit of 68%. To summarize, although the presence of F_2^{+**}-like CCs in LiF crystals increases the tuning range of wavelength-selective LiF : F_2^{+**} CC lasers, at low energy pumping the F_2^{+**}-like centers introduce passive losses of $\sim 0.08\ \text{cm}^{-1}$ at the oscillation wavelength. We believe these losses can be saturated at high pumping energies. Alternatively, the growth process of the LiF : F_2^{+**} CC crystals could be optimized to minimize the concentration of F_2^{+**}-like centers, but

this would limit the tuning range of the CC laser. Care is needed to balance these considerations when designing a LiF : F_2^{+**} CC laser in order to obtain the desired tuning range, efficiency, and range of pumping energies.

4. Amplification of narrow line LiF : F_2^{+**} laser oscillation

The main goal of this work was to study amplification of narrow-line LiF : F_2^{+**} CC laser emission in order to develop a tunable source of high-energy nanosecond laser pulses in the near-infrared. The near-infrared emission could then be frequency-doubled to provide a source in the visible range suitable for nanosecond nonlinear optics experiments.

The primary oscillator in this work was a tunable LiF : F_2^{+**} CC laser operated in a Littrow configuration. This oscillator design provided wide tunability, a narrow spectral line and high laser efficiency, along with a variety of possible pump wavelengths [1]. However, at reasonable pump energies, the output energy was insufficient for many nonlinear-optical applications. When the pump energy was increased, the spatial beam quality decreased and the spectral linewidth of the LiF : F_2^{+**} laser broadened, which is undesirable. In order to increase the usable pulse energy and still maintain the narrow linewidth and good spatial quality of the output pulses from the tunable LiF : F_2^{+**} CC laser, a two-stage oscillator–amplifier configuration was designed.

The optical arrangement of the two-stage system is shown in Fig. 5. The pump beam (633 nm, 7-ns pulses at 10-Hz repetition rate, as described above) was split into two channels at beam splitter BS1. Approximately 10% of the pump beam was used to pump the laser oscillator, and the rest was sent to the amplifier crystal. The laser oscillator pump beam passed through a 4× beam compressing telescope (T1) before being coupled into the laser cavity via flat mirror M1. The pump beam diameter was ~2.5 mm at the laser crystal. The laser cavity was 19 cm long and contained the 27-mm LiF : F_2^+ CC laser crystal. The laser crystal absorption was 1.97 cm^{-1} at the 600-nm

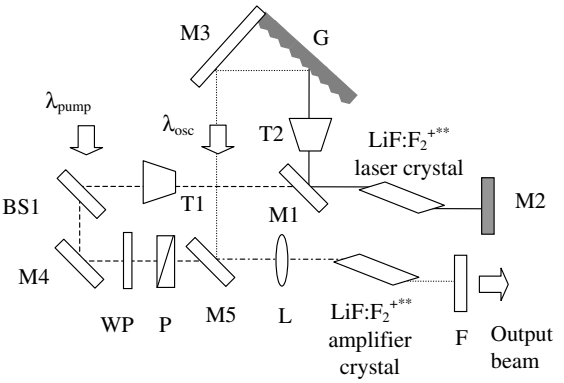

Fig. 5. Experimental set-up of the LiF : F_2^{+**} color center laser and amplifier.

absorption peak and 1.8 cm^{-1} at the pump wavelength of 633 nm. The cavity was formed by mirror M2 and a diffraction grating (G, 1200 grooves/mm) with diffraction efficiency of $R \approx 50\%$ operating in the autocollimation regime. The zeroth order of diffraction served for oscillation output. A 3× telescope (T2) expanded the beam before the diffraction grating in order to achieve higher resolution and prevent damage to the grating. Tuning of the output wavelength was accomplished by rotating the corner reflector formed by the grating and mirror M3. The LiF : F_2^{+**} CC laser efficiency at the maximum of the tuning curve (near 930 nm) was ~20%. The peak emission wavelength was determined largely by the reflectivity of the mirror M2. As shown in Fig. 6, the pulses emitted by the

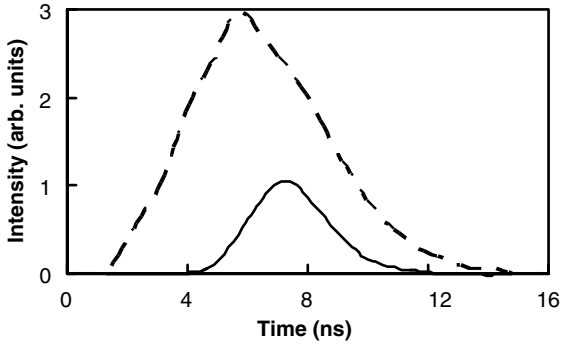

Fig. 6. Temporal profiles of the 633-nm pump pulse (dashed line) and output of a tunable LiF : F_2^{+**} laser cavity (solid line) measured with a fast photodiode detector.

oscillator overlap in time with the 7-ns pump pulses and are slightly shorter than the pump pulses in duration [19].

For amplification, the emission from the master laser oscillator and the remainder of the pump beam were coupled together at mirror M5 and focused colinearly into the Brewster-cut 38-mm LiF : F_2^{+**} CC amplifier crystal. The amplifier crystal absorption was 2.8 cm^{-1} at the 600-nm absorption peak and 2.5 cm^{-1} at the 633-nm pump wavelength. The position of the amplifier crystal after the 1-m focusing lens (L) was chosen to create high pump power densities in the crystal while avoiding the excitation of broadband superluminescence under maximum pump energy. The energy of the pump beam was attenuated using a quarter wave plate (WP) and polarizer (P) combination. The pump beam diameter in the crystal was ~2 mm, and the diameter of the seed beam from the LiF : F_2^{+**} CC laser was ~1.5 mm. After a single pass through the amplifier crystal, the remaining 633-nm pump light was absorbed by a dichroic filter (F).

Fig. 7 shows the output energy after the dichroic filter as a function of pump energy absorbed by the amplifier crystal for two levels of input energy from the laser oscillator. As shown in the figure, the slope efficiency is higher when 0.4 mJ seeding energy from the laser oscillator is used ($\eta = 32\%$) than when 0.33 mJ of seeding energy is used ($\eta = 26\%$). We find that the single-pass optical amplification ($G = E_{out}/E_{in}$) is linearly proportional to the absorbed pump energy density with a slope of 0.025 cm^2 mJ^{-1} regardless of whether 0.33 or 0.4 mJ of input energy is used. The maximum achieved amplification is $G = 37.5$ with 47 mJ absorbed pump energy and 0.4 mJ input energy. No saturation of the amplification process is observed, indicating that further increasing the pump energy should increase the amplification and the output energy.

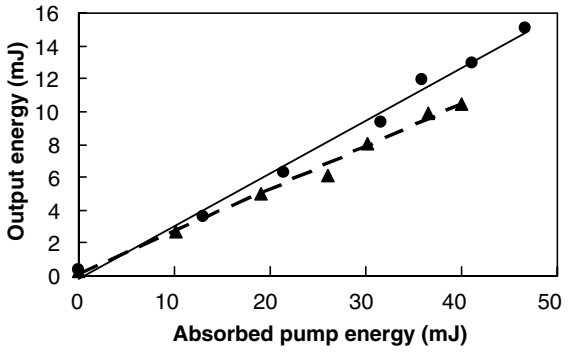

Fig. 7. Output energy as a function of absorbed pump energy for single pass amplification with input energy $E_{in} = 0.33$ mJ (triangles) and $E_{in} = 0.40$ mJ (circles). The dashed and solid lines are linear fits to the data, respectively.

5. Conclusions

To our knowledge, this paper presents the first implementation of a nanosecond master oscillator/power amplifier scheme using LiF : F_2^{+**} color center laser and amplifier crystals. The two-stage scheme is designed to yield high-energy output pulses while maintaining the spatial and spectral characteristics of the tunable LiF : F_2^{+**} CC laser. With input energies of 0.3–0.4 mJ, we achieve amplification of more than 35× under less than 50 mJ of absorbed pump energy. The single-pass optical amplification is found to be linearly proportional to the amplifier pump energy density with a slope of 0.025 cm^2 mJ^{-1}. This two-stage configuration yields nanosecond output pulse energies up to 15 mJ at wavelengths near 930 nm. These pulses could be frequency-doubled to create a tunable nanosecond source of visible light.

Additional improvements to the master oscillator/power amplifier system should be possible. For example, saturating the passive losses in the amplifier crystal by using higher-energy pump pulses could lead to a marked increase in amplifier gain. In addition, optimizing the temporal overlap between the pump and seed pulses in the amplifier crystal should also increase the amplifier gain.

We also present details related to the preparation of the LiF : F_2^{+**} CC crystals and measurement of passive losses in these crystals. Optimization of the coloration parameters for large-scale LiF crystals has enabled us to achieve the highest absorption coefficient to date in LiF : F_2^{+**} CCs (8 cm^{-1} at ~600 nm). In addition, we show that the concentration of F_2^{+**} CCs increases approximately exponentially during

room-temperature storage with an effective time constant of 3 months. Using Caird et al. [17] and Findlay–Clay [18] analysis, the non-saturated passive losses of a LiF : F_2^{+**} CC crystal in a non-selective cavity were found to be 0.08 cm^{-1} or less in the near infrared when the absorbed laser pump energy is below 20 mJ. We believe that these losses are related to absorption by F_2^{+**}-like color centers and that they can be saturated at high pump energies. This information will be useful for designing more efficient tunable lasers and amplifier systems based on LiF : F_2^{+**} color center crystals.

Acknowledgments

The authors thank Wei Qiu for preliminary work on the LiF : F_2^{+**} color center laser and Neil Jenkins for assistance with temporal pulse length measurements. This work was supported under Army Research Office Grants DAAD19-99-1-0119 and DAAD19-03-1-0218 and a Research Agreement between Light Age, Inc., and the University of Alabama at Birmingham.

References

[1] A.Yu. Dergachev, S.B. Mirov, Opt. Commun. 147 (1998) 107.
[2] V.V. Ter-Mikirtychev, Opt. Laser Technol. 30 (1998) 229.
[3] T.T. Basiev, S.B. Mirov, in: V.S. Letokhov, C.V. Shank, Y.R. Shen, H. Walther (Eds.), Laser Science and Technology, vol. 16, Harwood Academic Publishers, Chur, Switzerland, 1994, and references therein.
[4] V.M. Khulugurov, B.D. Lobanov, Sov. Tech. Phys. Lett. 4 (1978) 1471.
[5] A.E. Siegman, Lasers, University Science Books, Sausalito, CA, 1986.
[6] A.A. Hnilo, O.E. Martinez, IEEE J. Quantum Electron. QE-23 (1987) 593.
[7] A.A. Hnilo, F.A. Manzano, O.E. Martinez, J. Opt. Soc. Am. B 4 (1987) 629.
[8] T.E. Sharp, C.B. Dane, D. Barber, F.K. Tittel, P.J. Wisoff, G. Szabó, IEEE J. Quantum Electron. 27 (1991) 1221.
[9] M.J. Dyer, H. Helm, J. Opt. Soc. Am. B 10 (1993) 1035.
[10] D.Q. Hoa, N.D. Hung, J. Moroe, N. Takeyasu, T. Imasaka, Appl. Phys. Lett. 82 (2003) 3391.
[11] T.T. Basiev, I.V. Ermakov, V.A. Konyushkin, K.K. Pukhov, M. Glasbeek, Quantum Electron. 28 (1998) 179.
[12] T.T. Basiev, I.V. Ermakov, V.A. Konyushkin, K.K. Pukhov, Quantum Electron. 31 (2001) 424.
[13] V.A. Arkhangel'skaya, E.V. Guseva, G.M. Zinger, N.E. Korolev, V.M. Reiterov, Optik. Spektroskop. 61 (1986) 542 [Opt. Spectrosc. (USSR) 61 (1986) 340].
[14] N.A. Ivanov, V.D. Lokhnygin, A.A. Fomichev, V.M. Hulugurov, Sov. J. Quantum Electron. 16 (1986) 1645.
[15] V.V. Ter-Mikirtychev, J. Phys. Chem. Solids 58 (1997) 893.
[16] N.W. Jenkins, S.B. Mirov, V.V. Fedorov, J. Lumin. 91 (2000) 147.
[17] J.A. Caird, S.A. Payne, P.R. Staver, A.J. Ramponi, L.L. Chase, W.F. Krupke, IEEE J. Quantum Electron. 24 (1988) 1077.
[18] D. Findlay, R.A. Clay, Phys. Lett. 20 (1966) 277.
[19] N.W. Jenkins, "Spectroscopic properties and mechanisms of superbroadband lasing from F_2^{+**} color centers in LiF," dissertation, University of Alabama at Birmingham, 2000.